

SSM Meets Video Diffusion Models: Efficient Long-Term Video Generation with Selective State Spaces

Yuta Oshima^a, Shohei Taniguchi^a, Masahiro Suzuki^a, Yutaka Matsuo^a

^a*The University of Tokyo, 7-3-1, Hongo, Bunkyo-ku, Tokyo, Japan*

Abstract

Given the remarkable achievements in image generation through diffusion models, the research community has shown increasing interest in extending these models to video generation. Recent diffusion models for video generation have predominantly utilized attention layers to extract temporal features. However, attention layers are limited by their computational costs, which increase quadratically with the sequence length. This limitation presents significant challenges when generating longer video sequences using diffusion models. To overcome this challenge, we propose leveraging state-space models (SSMs) as temporal feature extractors. SSMs (e.g., Mamba) have recently gained attention as promising alternatives due to their linear-time memory consumption relative to sequence length. In line with previous research suggesting that using bidirectional SSMs is effective for understanding spatial features in image generation, we found that bidirectionality is also beneficial for capturing temporal features in video data, rather than relying on traditional unidirectional SSMs. We conducted comprehensive evaluations on multiple long-term video datasets, such as MineRL Navigate, across various model sizes. For sequences up to 256 frames, SSM-based models require less memory to achieve the same FVD as attention-based models. Moreover, SSM-based models often deliver better performance with comparable GPU memory usage. Our codes are available at <https://github.com/shim0114/SSM-Meets-Video-Diffusion-Models>.

Keywords: video generation, diffusion models, state-space models

1. Introduction

Research on video generation using diffusion models [56, 46, 29] is cutting-edge in the field of deep generative models. The success of image generation

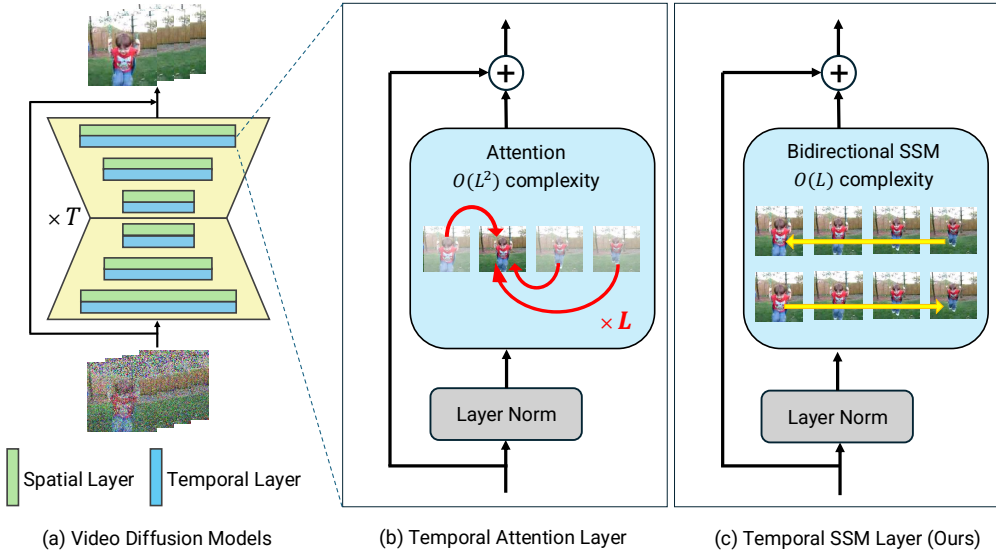


Figure 1: (a) U-Net based video diffusion models consist of spatial layers and temporal layers. (b) Conventional approaches use attention mechanisms in temporal layers, leading to quadratic growth in memory allocation and computational time as sequence length L increases. (c) We propose using SSMs in temporal layers, where memory allocation and computational time increase only linearly with sequence length L .

using diffusion models, notably Denoising Diffusion Probabilistic Models (DDPMs) [29], has sparked a surge in research on applying diffusion models to video generation. This trend has been exemplified by the emergence of video diffusion models (VDMs) [31]. By harnessing the substantial representational capacity inherent in diffusion models, their application to video generation has showcased impressive performance in modeling the dynamic and intricate nature of video content [31, 54, 30].

However, research on diffusion-model-based video generation faces significant challenges in terms of computational complexity with respect to video sequence length. In diffusion models for video generation, attention mechanisms [61] are employed to capture temporal relationships [31, 54, 30, 70, 3]. In early studies on diffusion models for video generation, such as VDMs, to capture temporal relationships across video frames, temporal attention layers were added after spatial attention layers within the architecture of diffusion models for image generation, as described in Figure 1(a)(b). However, the memory demands of attention layers, which scale with the square of the sequence length, present

substantial challenges for extending these models to handle longer sequences. Consequently, current research predominantly focuses on short-term video generation, typically around 16 frames per inference [31, 54, 3], which equates to less than a second of video at 30 fps.

Recently, state-space models (SSMs) [21, 22, 23, 55], especially Mamba [20], have been identified as promising alternatives to attention mechanisms. In contrast to attention mechanisms, SSMs can handle sequential data with linear complexities, so they are expected to overcome the fundamental limitation of attention-based models in many sequence modeling tasks. Subsequent studies have also shown that SSMs are effective alternatives to attention-based approaches across various domains (see section 4.2).

A key finding from our investigation is that, in the context of video generation, adopting a bidirectional approach allows SSMs to more comprehensively understand the temporal dynamics in video data (Figure 1(c)). This finding aligns with previous research showing that incorporating SSMs that observe various directions enhances the generation quality of models capturing spatial dependencies in images [67, 33, 13]. Notably, our empirical observations reveal that a naive replacement of temporal attention layers in VDMs with unidirectional SSMs significantly underperforms compared to the original attention-based VDMs.

We first conducted experiments on MineRL Navigate dataset [24, 52], a widely used long-term video dataset, varying the number of frames to 16, 64, and 256, to compare the computational cost and video generation quality of SSM-based models with attention-based models. For long sequences of 256 frames, we found that SSM-based models, even with larger model sizes, can be trained with similar memory usage as attention-based models. This results in reduced memory requirements to achieve the same FVD as attention-based models. Furthermore, when the GPU memory usage is comparable, SSM-based models often outperform attention-based models in terms of performance. The effectiveness of SSM-based models at 256 frames was also confirmed on several long-term video datasets, including GQN-Mazes [12, 52] and CARLA Town01 [9, 25].

2. Background

In this section, we provide an overview of our initial understanding of diffusion models for video generation. Diffusion models were initially introduced by Sohl-Dickstein et al. [56], and Ho et al. [29] further advanced the field with the

introduction of denoising diffusion probabilistic models (DDPMs). DDPMs introduced a practical training algorithm, particularly well-suited for image generation. Recent advancements in diffusion models for video generation involve the extension of the DDPM architecture to accommodate video data.

2.1. Denoising Diffusion Probabilistic Models (DDPMs)

In diffusion models, the forward process involves progressively diminishing the original data signal, \mathbf{x}_0 , by gradually introducing Gaussian noise as the diffusion time, t , advances. This sequence of transformations leads \mathbf{x}_0 to converge to pure Gaussian noise, represented as $\mathbf{x}_T \sim \mathcal{N}(\mathbf{x}_T; \mathbf{0}, \mathbf{I})$, at time T . In our study, t is treated as a discrete integer within the range $[0, T]$, although some studies have considered t as a continuous variable [57, 37]. The forward process is governed by the following following Markov process:

$$q(\mathbf{x}_{1:T} | \mathbf{x}_0) = \prod_{t=1}^T q(\mathbf{x}_t | \mathbf{x}_{t-1}), \quad (1)$$

$$q(\mathbf{x}_t | \mathbf{x}_{t-1}) = \mathcal{N}(\mathbf{x}_t; \sqrt{\alpha_t} \mathbf{x}_0, (1 - \alpha_t) \mathbf{I}). \quad (2)$$

In this formulation, the sequence σ_t satisfies $0 < \sigma_1 < \dots < \sigma_{T-1} < \sigma_T < 1$. The generation process in diffusion models is the reverse process. This process starts with pure Gaussian noise $\mathbf{x}_T \sim \mathcal{N}(\mathbf{x}_T; \mathbf{0}, \mathbf{I})$ and gradually reconstructing the data towards the original \mathbf{x}_0 . During the reverse process, each step $p_\theta(\mathbf{x}_{t-1} | \mathbf{x}_t)$ is modeled using a neural network.

$$p_\theta(\mathbf{x}_{1:T}) = p(\mathbf{x}_T) \prod_{t=1}^T p_\theta(\mathbf{x}_{t-1} | \mathbf{x}_t), \quad (3)$$

$$p_\theta(\mathbf{x}_{t-1} | \mathbf{x}_t) = \mathcal{N}(\mathbf{x}_{t-1}; \boldsymbol{\mu}_\theta(\mathbf{x}_t, t), \boldsymbol{\Sigma}_\theta(\mathbf{x}_t, t)), \quad (4)$$

$$p(\mathbf{x}_T) = N(\mathbf{x}_T; \mathbf{0}, \mathbf{I}). \quad (5)$$

Typically, $\boldsymbol{\Sigma}_\theta$ is set as an untrainable, time-dependent constant, $\boldsymbol{\Sigma}_\theta(\mathbf{x}_t, t) = \sigma_t \mathbf{I}$. Additionally, with a change in the parameterization of $\boldsymbol{\mu}_\theta$, the reverse process $p_\theta(\mathbf{x}_{t-1} | \mathbf{x}_t)$ can be expressed as:

$$\begin{aligned} & p_\theta(\mathbf{x}_{t-1} | \mathbf{x}_t) \\ &= \mathcal{N} \left(\mathbf{x}_{t-1}; \frac{1}{\sqrt{\alpha_t}} \left(\mathbf{x}_t + \frac{\sigma_t^2}{\sqrt{\alpha_t - 1}} \boldsymbol{\epsilon}_\theta(\mathbf{x}_t, t) \right), \sigma_t \mathbf{I} \right), \end{aligned} \quad (6)$$

where $\bar{\alpha}_t = \prod_{i=1}^t (1 - \sigma_i^2)$. The term $\epsilon_\theta(\mathbf{x}_t, t)$ represents a function that predicts the noise from noisy data \mathbf{x}_t . This parameterization results in an objective function for the DDPM structured as follows:

$$\mathbb{E}_{\mathbf{x}_0, \epsilon, t} [\|\epsilon - \epsilon_\theta(\mathbf{x}_t, t)\|_2^2], \quad (7)$$

where $\mathbf{x}_t = \sqrt{\bar{\alpha}_t} \mathbf{x}_0 + \sqrt{1 - \bar{\alpha}_t} \epsilon$. While numerous parameterizations are recognized, such as predicting the observed data \mathbf{x}_0 from its noisy counterpart \mathbf{x}_t or \mathbf{v} -prediction [31, 51, 37], we chose to utilize the ϵ -prediction.

In terms of the architecture of diffusion models, 2D U-Net [49] architectures are commonly used for image data. In 2D U-Net-based models, spatial attention layers are incorporated between the convolutional layers. These spatial attention layers enhance the ability to focus on relevant spatial features and improve the quality of the generated images. Although we adopted a U-Net-based architecture for the diffusion model, Peebles and Xie [47] explored architectures based on Vision Transformers (ViT) [10].

2.2. Architectures for Video Diffusion Models

To generate videos, diffusion models need to encapsulate both spatial and temporal features across frames. While DDPMs typically comprise a combination of U-Net and spatial attention layer, their capability is predominantly confined to spatial feature capture.

To address this limitation, Video Diffusion Models (VDMs) [31] were introduced as an initial attempt at video generation using diffusion models. By incorporating mechanisms to capture temporal dynamics within DDPMs, VDMs enhance their capability to capture temporal features (Figure 1 (a)(b)). Temporal attention layers are commonly used in video generation diffusion models, such as VDMs, to leverage time-series dependencies. However, temporal attentions require memory proportional to the square of the sequence length, which imposes limitations on the maximum length of video sequences that can be generated at once. In our study, we adopt VDMs as a baseline to explore the existing challenges and potential improvements in video generation using diffusion models.

3. Method

In this section, we propose the architecture of a temporal SSM (state-space model) layer for use in diffusion models for videos. Recent diffusion model-based video generation techniques capture temporal features through temporal

attention layers, incurring memory costs proportional to the square of the sequence length. Recently, SSMs have emerged as a promising alternative to attention, offering linear memory costs with respect to the sequence length [21, 22, 23, 55, 20]. We first review the recent advancements in SSMs in prior works, followed by a detailed description of our proposed temporal SSM layer architecture for video generation diffusion models.

3.1. State Space Models

Unlike the temporal attention commonly used in video diffusion models, state-space models (SSMs) enable the processing of time series with spatial complexities proportional to the sequence length. Recent studies proposed SSMs that could process inputs in parallel, unlike recurrent models such as recurrent neural networks (RNNs) [5].

SSMs are widely used as sequence models that define a mapping from one-dimensional input signals $u(t) \in \mathbb{R}$ to one-dimensional output signals $y(t) \in \mathbb{R}$, with $\mathbf{s}(t) \in \mathbb{R}^N$ representing the hidden state. Continuous time processes are formulated as follows:

$$\begin{aligned}\dot{\mathbf{s}}(t) &= \mathbf{A}\mathbf{s}(t) + \mathbf{B}u(t), \\ y(t) &= \mathbf{C}\mathbf{s}(t) + Du(t),\end{aligned}\tag{8}$$

where $\mathbf{A} \in \mathbb{R}^{N \times N}$, $\mathbf{B} \in \mathbb{R}^{N \times 1}$, $\mathbf{C} \in \mathbb{R}^{1 \times N}$ denote the diagonal state matrix, input matrix, and output matrix for hidden state respectively. $D \in \mathbb{R}$ is direct path from input to output.

For applying SSMs with real-world data, SSMs formulated as Equation 8 are converted into discrete versions utilizing the zero-order hold (ZOH) method [23]:

$$\begin{aligned}\mathbf{s}_k &= \bar{\mathbf{A}}\mathbf{s}_{k-1} + \bar{\mathbf{B}}u_k, \\ y_k &= \mathbf{C}\mathbf{s}_k + Du_k,\end{aligned}\tag{9}$$

where $\bar{\mathbf{A}} = \exp(\Delta \mathbf{A})$, $\bar{\mathbf{B}} = (\Delta \mathbf{A})^{-1}(\exp(\mathbf{A}) - \mathbf{I}) \cdot \Delta \mathbf{B}$ with Δ as the timescale parameter for ZOH.

Diversing from previous SSMs which are limited to linear time-invariant (LTI) systems, Mamba [20] introduces a selective scan mechanism (S6). In S6, the parameters $\mathbf{B} \in \mathbb{R}^{B \times L \times N}$, $\mathbf{C} \in \mathbb{R}^{B \times L \times N}$, $\Delta \in \mathbb{R}^{B \times L \times D}$ are dependent on input $\mathbf{u} \in \mathbb{R}^{B \times L \times D}$. This enables the model to selectively discard irrelevant information while retaining essential information over extended periods. Using

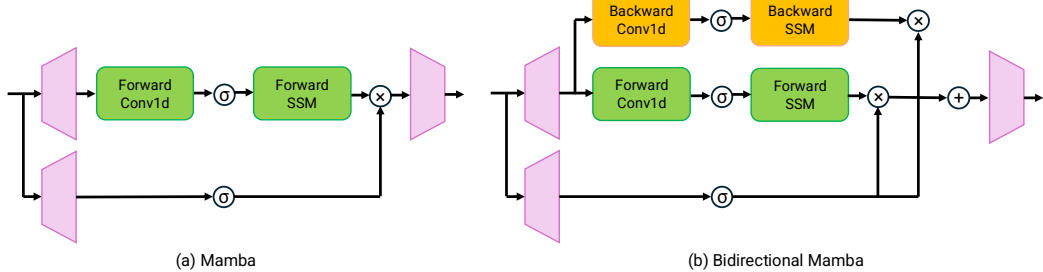


Figure 2: Architectural comparison of Mamba and bidirectional Mamba. Layer Normalization [1] and a skip connection [26] are omitted for simplicity.

an efficient scan algorithm, S6 is capable of parallel computation with linear complexity relative to the sequence length.

3.2. Temporal SSM Layer for Diffusion Model-based Video Generation

We incorporate state-space models (SSMs) within the temporal layers for the video generation diffusion model (Figure 1 (c)). In our model, we replace the self-attention component with an SSM and adopt a bidirectional SSM structure, drawing from practices in [18, 65]. This choice is motivated by the inherent limitation of a single SSM, which is typically restricted to capturing unidirectional temporal transitions. In models capturing spatial dependencies in images using SSMs, incorporating SSMs that observe various directions can enhance generation quality [67, 72, 41]. Similarly, we found that by adopting a bidirectional approach, SSMs can more comprehensively understand the temporal dynamics in video data.

We specifically chose to adopt the bidirectional Mamba architecture as proposed by [72] (Figure 2). Following the standard setup used in previous works on Mamba [20, 72, 41], we set the expansion factor of the input dimensions via linear projection to $E = 2$, the internal state dimension of the SSM to $N = 16$, and adopted SiLU [11] as the activation function. The input is denoted as $\mathbf{X} \in \mathbb{R}^{(B \times H \times W) \times L \times C}$, where L is the sequence length, C is the channel size, H is the height, and W is the width of the input image.

4. Related Works

4.1. Deep Generative Models for Video Generation

The field of video synthesis has seen significant advancements through various studies. Prior to the emergence of diffusion models, the use of generative

adversarial networks (GANs) [17] dominated the scene. These methods extended traditional image-GAN frameworks to video generation, focusing on enhancing their generative capabilities [63, 50, 59, 15]. These approaches primarily aimed to achieve their objectives by extending common architectures of GANs for image generation. Additionally, the development of long-term video generation techniques, particularly those leveraging the transitions of latent variables in variational autoencoders (VAEs) [36] are also well-known [35, 19, 52, 68].

The advent of diffusion models in image generation [56, 46, 29] marked a turning point, with their subsequent application to video distributions demonstrating promising outcomes [31, 54, 30, 25, 3]. These approaches have shown promising results. Nevertheless, the recent approaches adopt attention mechanisms to temporal layers, which require memory proportional to the square of the sequence length, the computational and memory demands of video-diffusion models pose a substantial challenge. To mitigate this, spatio-temporal downsampling [54, 30], utilizing latent features [48, 27, 70, 3] are proposed. In the realm of long-term video prediction using video diffusion models, multistep generation techniques stand out [62, 32, 25, 69]. These schemes generate videos through successive sampling with flexible frame conditioning, allowing for efficient long-term dependency modeling with minimal memory usage. Our research diverges from them by focusing on architectural improvements rather than sampling schemes.

4.2. SSMs and Their Applications

Mamba, a recent SSM introduced by Gu and Dao [20], offers efficient computation and demonstrates outstanding performance, in HiPPO [21] and S4 [22] laid the groundwork for subsequent advancements in sequence modeling frameworks, including the development of Mamba. By introducing a structured parameterization of SSMs, S4 enabled efficient computation and demonstrated exceptional performance in capturing long-range dependencies [58]. S4D [23] is a simplified version of S4 that introduced a diagonal matrix formulation. SSMs have been applied across various domains, including image and video classification [45, 39, 34, 64, 72, 41, 40], segmentation [43], speech generation [16], time-series generation [71], language modeling [44, 65, 6], reinforcement learning [2, 42, 7].

In the field of diffusion models using SSMs, DiffuSSM [67] have first explored the integration of SSMs with diffusion models, replacing the computationally intensive spatial attention mechanisms in image generation with SSMs. Other

Table 1: Model Configuration. The settings for the UNet-based diffusion models used in the experiments. The models are scaled such that the base channel size is proportional to the number of attention heads, while the attention hidden dimension is fixed at 64.

Attention-based Models					
Params	# Base channels	# Attention heads	# Attention dims	Spatial	Temporal
14.1M	32	4	64	Linear attn.	Attention
56.3M	64	8	64	Linear attn.	Attention
71.2M	72	9	64	Linear attn.	Attention
225M	128	16	64	Linear attn.	Attention
900M	256	32	64	Linear attn.	Attention
SSM-based Models					
Params	# Base channels	# Attention heads	# Attention dims	Spatial	Temporal
14.5M	32	4	64	Linear attn.	SSM
57.5M	64	8	64	Linear attn.	SSM
175M	112	14	64	Linear attn.	SSM
229M	128	16	64	Linear attn.	SSM
913M	256	32	64	Linear attn.	SSM

studies have also explored replacing spatial attention with SSMs for image generation, as well as handling spatio-temporal information globally for short-term video generation (e.g., 16 frames) [33, 14, 13]. In contrast, our research differentiates itself by replacing the temporal attention in video generation models with Mamba, aiming to generate longer-term videos (e.g., 256 frames).

5. Experiments

In this section, we conducted a series of experiments demonstrating that incorporating SSMs into diffusion models for video generation effectively captures temporal dependencies, particularly in generating long-term videos (e.g., 256 frames), while maintaining computational efficiency. Our experiments across multiple datasets and various settings revealed that, under equivalent memory usage, temporal SSMs outperformed in generating long-term videos. These findings suggest that utilizing SSMs in temporal layers is beneficial for constructing video diffusion models capable of long-term video generation under constrained computational resources.

5.1. Experimental Setup

Models For each experimental setup, we conducted experiments using both VDMs with temporal attention layers and VDMs with SSM-based temporal layers, across multiple model sizes. The number of parameters and scaling methods for each model are detailed in Table 1 . The model size for generating 256-frame long videos was selected based on the scaling approach used in this study, ensuring that the experiments were feasible within the constraints of the available hardware, which comprised eight NVIDIA A100 GPUs (40 GB each). The VDMs were implemented based on a publicly available and widely used implementation ¹ that utilizes UNet’s convolution layer and linear attention [53, 38, 66] for capturing spatial features. In this paper, we focused on comparing only the layers responsible for capturing temporal features, as changes in the spatial feature extraction are not relevant to our investigation.

Datasets We first utilized the MineRL Navigate dataset [24, 52], a commonly used dataset for long-term video generation, derived from the Minecraft environment. The training set consisted of a total of 1,186 videos, combining both the train and test splits. We trained our models using videos with varying frame lengths of 16, 64, and 256 frames to evaluate the computational cost and generative performance when using SSMs versus attention as the temporal layer under different frame lengths. Additionally, we employed the GQN-Mazes [12, 52] and CARLA-Town01 [9, 25] datasets for long-term video generation tasks. The GQN-Mazes dataset contains 108,200 videos from a 3D maze simulator environment, while the CARLA Town01 dataset includes 508 videos from a driving simulator environment. For these datasets, we trained our models using videos with 256 frames. Across all experiments, the spatial resolution of the videos was fixed at 32x32 pixels. Training details for each dataset and each frame length are shown in Appendix Appendix A.

Baseline We established our experimental baseline using VDMs [31]. Our analysis was meticulously designed to alter only the temporal attention layers in VDMs with our temporal SSM layers. This strategy enabled a focused examination of the impact and efficacy of the temporal SSM layers in the context of video generation, facilitating a direct comparison with the existing temporal layers.

Evaluation Metrics In our validation process, we evaluated the sample quality of the videos generated by the trained models. To evaluate the

¹<https://github.com/lucidrains/video-diffusion-pytorch>

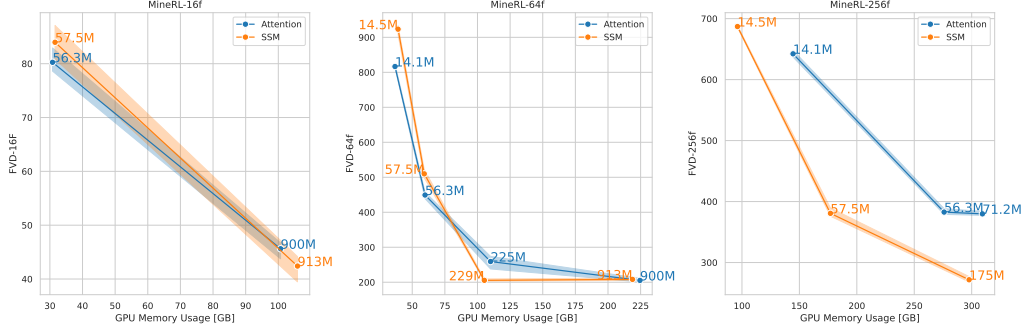


Figure 3: Comparison of GPU memory usage and FVD between the temporal SSM layer and temporal attention on the MineRL Navigate dataset: 16 frames (left), 64 frames (center), 256 frames (right). Each plot point includes the model size next to it.

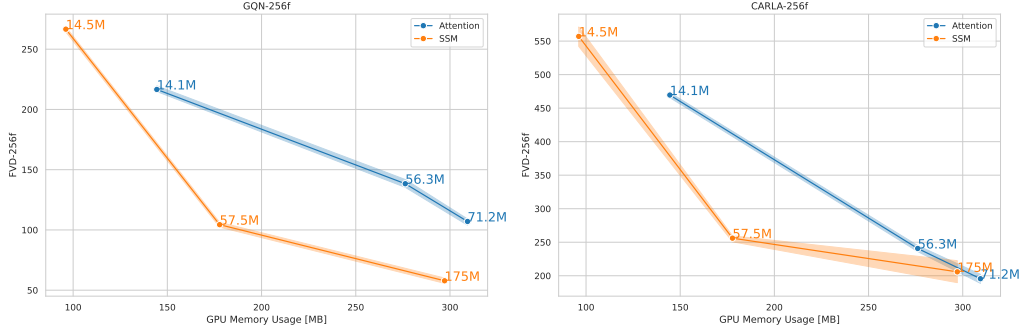


Figure 4: Comparison of GPU memory usage and FVD between the temporal SSM layer and temporal attention for 256 frames on the GQN-Mazes (left) and CARLA Town01 (right) datasets. Each plot point includes the model size next to it.

quality of the generated videos, we employ the Fréchet Video Distance (FVD) metric [60], using an I3D network pretrained on the Kinetics-400 dataset [4]. FVD is a recognized standard for assessing the quality of generated videos [31, 15, 54, 30, 25], where lower scores denote superior quality. For the MineRL Navigate dataset, the calculations involve all 1,186 videos and 1,000 generated samples. For the GQN-Mazes dataset, the calculations involve 2,000 videos from the dataset and 2,000 generated samples, while for the CARLA Town01 dataset, all 508 videos from the dataset and 500 generated samples are used. We used three different random seeds to introduce variation in data sampling and sample generation for FVD calculation.

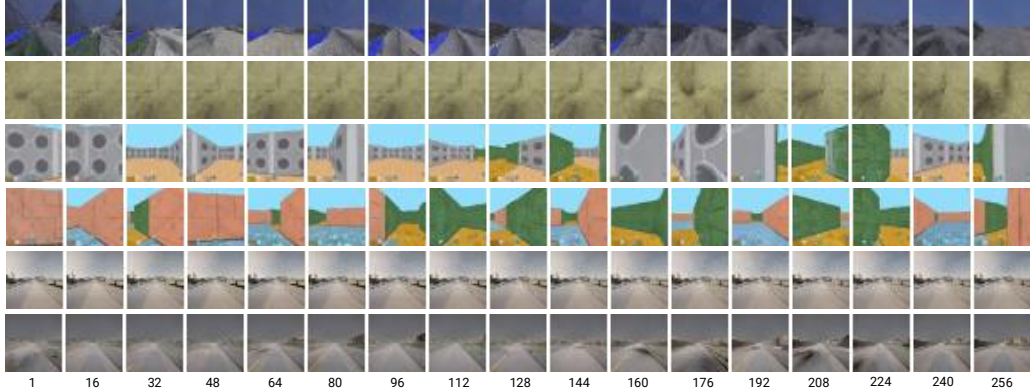


Figure 5: Videos generated by temporal SSM-based VDMs. Each column represents different samples, with the top two rows corresponding to MineRL Navigate, the middle two to GQN-Mazes, and the bottom two to CARLA Town01 (# of frames are 256, 32×32 resolution). Additional qualitative results are provided in Figure B.7, B.8, B.9.

5.2. Main Results

We trained models of various sizes across different settings, with the results shown in Figure 3 and 4, and Table 2 and 3. First, we describe the results obtained from the MineRL Navigate dataset with varying video frames. For sequences of 16 and 64 frames, the VDM with an SSM-based temporal layer demonstrates comparable generative performance to that of the attention-based temporal layer. However, when the frame count increases to 256 frames, the SSM-based VDM exhibits superior generative performance relative to memory usage compared to the attention-based approach. Furthermore, experiments conducted on the GQN-Mazes and CARLA Town01 datasets confirm the advantages of using an SSM-based temporal layer in VDMs over attention-based layers. These benefits, particularly in terms of generative performance relative to memory usage, extend beyond the MineRL Navigate dataset. This advantage is especially evident in the generation of 256-frame video sequences across various scenarios. The generated samples from temporal SSM-based VDMs are shown in Figure 5.

In Figure 6, we present how training memory consumption and inference time vary with video sequence length for each temporal layer, using 32×32 resolution images and the same model size. Training memory consumption data is based on a batch size of 8, while inference times reflect sample generation on a single NVIDIA A100 GPU with the number of diffusion time steps T fixed at 256. The results for 256 frames are particularly notable,

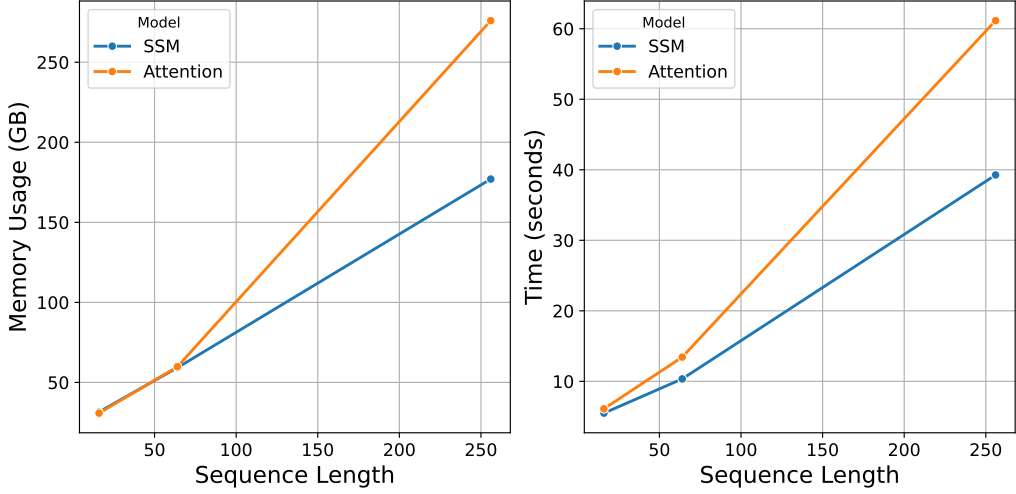


Figure 6: Left: Memory consumption during training with 8 NVIDIA A100 GPUs (40 GB) at a batch size of 8 and resolution of 32×32 . Right: Inference time for generating a sample with a single NVIDIA A100 GPU at a resolution of 32×32 and $T = 256$.

demonstrating that while memory usage and inference speed in Attention-based models increase quadratically with sequence length, the SSM-based model exhibits only a linear increase.

The results of this experiment suggest that SSMs can serve as a viable alternative to attention mechanisms in the temporal layers, even for the generation of relatively short videos, such as those with 16 or 64 frames. Furthermore, in the generation of longer videos, such as those with 256 frames, SSM-based models can achieve higher-quality video generation compared to attention-based models. This is because SSMs allow for larger model sizes while maintaining comparable computational resources. Additionally, this trend is expected to become more pronounced as the number of video frames increases, based on the observed relationship between the number of frames and computational cost.

5.3. Bidirectionality of Temporal SSM Layers

Our ablation study revealed that bidirectional processing within the SSM is crucial for generating high-quality videos when capturing temporal features in video sequences. Specifically, in our experiments with 256-frame video generation on the MineRL Navigate dataset, using a unidirectional SSM led to a significant decline in generative quality (Table 4).

Table 2: Quantitative results of experiments in MineRL Navigate. Memory consumption during training with 8 NVIDIA A100 GPUs (40 GB) at a batch size of 8 and resolution of 32×32 . Inference time for generating a sample with a single NVIDIA A100 GPU at a resolution of 32×32 and $T = 256$.

16 frames			
Models	Memory Usage	Inference Time	FVD-16f ↓
Attention-56.3M	30.8 GB	6.11 sec.	80.3
Attention-900M	101 GB	18.2 sec.	45.6
SSM-57.5M	31.6 GB	5.49 sec.	84.0
SSM-913M	106 GB	20.6 sec.	42.4
64 frames			
Models	Memory Usage	Inference Time	FVD-64f ↓
Attention-14.1M	36.8 GB	8.19 sec.	817
Attention-56.3M	59.8 GB	13.4 sec.	449
Attention-225M	110 GB	29.5 sec.	259
Attention-900M	224 GB	68.1 sec.	205
SSM-14.5M	36.8 GB	5.76 sec.	923
SSM-57.5M	59.2 GB	10.3 sec.	510
SSM-229M	105 GB	23.3 sec.	205
SSM-913M	219 GB	50.9 sec.	208
256 frames			
Models	Memory Usage	Inference Time	FVD-256f ↓
Attention-14.1M	144 GB	29.6 sec.	642
Attention-56.3M	276 GB	61.1 sec.	383
Attention-71.2M	309 GB	70.8 sec.	380
SSM-14.5M	96.1 GB	19.2 sec.	687
SSM-57.5M	177 GB	39.3 sec.	381
SSM-175M	298 GB	76.6 sec.	272

This finding suggests that treating time non-causally is preferable in fixed-length video generation models. It is well-known that in image generation diffusion models using SSMs, performance improvements are achieved by employing SSMs that process multiple directions in the spatial domain [67, 33, 13]. This behavior is rooted in the fact that SSMs are inherently causal information processing mechanisms. Our ablation results indicate that a similar approach—avoiding purely causal processing—also benefits the temporal domain in video generation.

Table 3: Quantitative results of experiments in GQN-Mazes and CARLA Town01.

GQN-Mazes 256 frames			
Models	Memory Usage	Inference Time	FVD-256f ↓
Attention-14.1M	144 GB	29.6 sec.	217
Attention-56.3M	276 GB	61.1 sec.	138
Attention-71.2M	309 GB	70.8 sec.	107
SSM-14.5M	96.1 GB	19.2 sec.	267
SSM-57.5M	178 GB	39.3 sec.	104
SSM-175M	297 GB	76.6 sec.	57.8
CARLA Town01 256 frames			
Models	Memory Usage	Inference Time	FVD-256f ↓
Attention-14.1M	145 GB	29.6 sec.	470
Attention-56.3M	276 GB	61.1 sec.	241
Attention-71.2M	309 GB	70.8 sec.	196
SSM-14.5M	96.1 GB	19.2 sec.	557
SSM-57.5M	178 GB	39.3 sec.	256
SSM-175M	297 GB	76.6 sec.	206

Table 4: Performance comparison of bidirectional SSM and unidirectional SSM.

Bidirectional	Params	Memory	Inference Time	FVD-256f ↓
✓	57.5 M	177 GB	39.3 sec.	381
	56.9 M	146 GB	31.8 sec.	610

6. Discussion

Our experimental findings demonstrate that incorporating SSM into the temporal layers of diffusion models for video generation offers superior video modeling in terms of memory efficiency for handling increased sequence lengths compared to traditional models employing temporal attention, while maintaining competitive generative quality. It is empirically shown that, compared to attention-based models, SSM-based video diffusion models can be scaled to larger sizes under the same computational cost, leading to higher-quality video generation for longer sequences. These outcomes underscore the adaptability of temporal SSM layers in enhancing video diffusion models and indicate their extensive potential impact on future advancements in this domain.

This study paves the way for numerous future investigations. While we have verified the advantages of employing our temporal SSM layers within the architecture of VDMs, the application of our temporal SSM layers extends beyond this, to any model that employs temporal attention for temporal dimension. For example, adopting temporal SSM layers into the temporal components of architectures such as Make-A-Video [54] or Imagen Video [30] could further enhance their computational efficiency by leveraging their existing spatiotemporal downsampling mechanism. Additionally, the combination of the temporal SSM layers with Latent Diffusion Models [48] could lead to significant reductions in computational costs. Our findings also offer insights for methods that involve freezing pretrained image-generation diffusion models and training new temporal layers for video generation; simply substituting these newly inserted temporal layers with the SSM layers could be an effective strategy. Moreover, while our experiments concentrated on unconditional video generation, integrating our approach with conditional generation techniques such as classifier guidance [8] and classifier free guidance [28] could pave the way for more efficient text-to-video (T2V) models.

The results of this study indicate that the incorporation of SSMs can lead to the development of long-term video generation models that demand fewer memory resources. This has noteworthy implications for broadening the accessibility of cutting-edge research in video generation diffusion models. Even institutions with limited computational resources can engage in this advanced field, potentially expediting the pace of research and innovation in video generation.

References

- [1] J. L. Ba, J. R. Kiros, and G. E. Hinton. Layer normalization. *arXiv preprint arXiv:1607.06450*, 2016.
- [2] Shmuel Bar David, Itamar Zimerman, Eliya Nachmani, and Lior Wolf. Decision s4: Efficient sequence-based rl via state spaces layers. In *International Conference on Learning Representations*, 2023.
- [3] Andreas Blattmann, Robin Rombach, Huan Ling, Tim Dockhorn, Seung Wook Kim, Sanja Fidler, and Karsten Kreis. Align your latents: High-resolution video synthesis with latent diffusion models. In *CVPR*, 2023.

- [4] J. Carreira and A. Zisserman. Quo vadis, action recognition? a new model and the kinetics dataset. In *CVPR*, 2017.
- [5] Junyoung Chung, Caglar Gulcehre, KyungHyun Cho, and Yoshua Bengio. Empirical evaluation of gated recurrent neural networks on sequence modeling. *arXiv preprint arXiv:1412.3555*, 2014.
- [6] Tri Dao, Daniel Y Fu, Khaled K Saab, Armin W Thomas, Atri Rudra, and Christopher Ré. “hungry hungry hippos: Towards language modeling with state space models”. In *The International Conference on Learning Representations (ICLR)*, 2023.
- [7] Fei Deng, Junyeong Park, and Sungjin Ahn. Facing off world model backbones: Rnns, transformers, and s4. *arXiv:2307.02064*, 2023.
- [8] Prafulla Dhariwal and Alex Nichol. Diffusion models beat gans on image synthesis. *arXiv preprint arXiv:2105.05233*, 2021.
- [9] Alexey Dosovitskiy, German Ros, Felipe Codevilla, Antonio Lopez, and Vladlen Koltun. Carla: An open urban driving simulator. In *Conference on Robot Learning*, pages 1–16. PMLR, 2017.
- [10] Alexey Dosovitskiy, Lucas Beyer, Alexander Kolesnikov, Dirk Weissenborn, Xiaohua Zhai, Thomas Unterthiner, Mostafa Dehghani, Matthias Minderer, Georg Heigold, Sylvain Gelly, et al. An image is worth 16x16 words: Transformers for image recognition at scale. *arXiv preprint arXiv:2010.11929*, 2020.
- [11] Stefan Elfwing, Eiji Uchibe, and Kenji Doya. Sigmoid-weighted linear units for neural network function approximation in reinforcement learning. *Neural Networks*, 107:3–11, 2018.
- [12] SM Ali Eslami et al. Neural scene representation and rendering. *Science*, 360(6394):1204–1210, 2018.
- [13] Yunxiang Fu, Chaoqi Chen, and Yizhou Yu. Lamamba-diff: Linear-time high-fidelity diffusion models based on local attention and mamba. *arXiv preprint arXiv:2408.02615*, 2024.
- [14] Yu Gao et al. Matten: Video generation with mamba-attention. *arXiv preprint arXiv:2405.03025*, 2024.

- [15] Songwei Ge, Thomas Hayes, Harry Yang, Xi Yin, Guan Pang, David Jacobs, Jia-Bin Huang, and Devi Parikh. Long video generation with time-agnostic vqgan and time-sensitive transformer. *arXiv preprint arXiv:2204.03638*, 2022.
- [16] Karan Goel, Albert Gu, Chris Donahue, and Christopher Ré. It’s raw! audio generation with state-space models. In *International Conference on Machine Learning*, 2022.
- [17] Ian Goodfellow, Jean Pouget-Abadie, Mehdi Mirza, Bing Xu, David Warde-Farley, Sherjil Ozair, Aaron Courville, and Yoshua Bengio. Generative adversarial nets. In *Advances in Neural Information Processing Systems*, pages 2672–2680, 2014.
- [18] Alex Graves and Jürgen Schmidhuber. Framewise phoneme classification with bidirectional lstm and other neural network architectures. *Neural Networks*, 18(5-6):602–610, 2005.
- [19] K. Gregor and F. Besse. Temporal difference variational auto-encoder. *arXiv preprint arXiv:1806.03107*, 2018.
- [20] Albert Gu and Tri Dao. Mamba: Linear-time sequence modeling with selective state spaces. *arXiv preprint arXiv:2312.00752*, 2023.
- [21] Albert Gu, Tri Dao, Stefano Ermon, Atri Rudra, and Christopher Ré. Hippo: Recurrent memory with optimal polynomial projections. *Advances in Neural Information Processing Systems*, 33:1474–1487, 2020.
- [22] Albert Gu, Karan Goel, and Christopher Ré. Efficiently modeling long sequences with structured state spaces. *arXiv preprint arXiv:2111.00396*, 2021.
- [23] Albert Gu, Karan Goel, Ankit Gupta, and Christopher Ré. On the parameterization and initialization of diagonal state space models. In *Advances in Neural Information Processing Systems*, volume 35, pages 35971–35983, 2022.
- [24] William H Guss, Brandon Houghton, Nicholay Topin, Phillip Wang, Cayden Codel, Manuela Veloso, and Ruslan Salakhutdinov. Minerl: A large-scale dataset of minecraft demonstrations. *arXiv preprint arXiv:1907.13440*, 2019.

- [25] William Harvey, Saeid Naderiparizi, Vaden Masrani, Christian Weilbach, and Frank Wood. Flexible diffusion modeling of long videos. *arXiv preprint arXiv:2205.11495*, 2022.
- [26] Kaiming He et al. Deep residual learning for image recognition. In *Proceedings of the IEEE conference on computer vision and pattern recognition*, 2016.
- [27] Yingqing He et al. Latent video diffusion models for high-fidelity long video generation. *arXiv preprint arXiv:2211.13221*, 2022.
- [28] Jonathan Ho and Tim Salimans. Classifier-free diffusion guidance. *arXiv preprint arXiv:2207.12598*, 2022.
- [29] Jonathan Ho, Ajay Jain, and Pieter Abbeel. Denoising diffusion probabilistic models. In *Advances in Neural Information Processing Systems*, pages 6840–6851, 2020.
- [30] Jonathan Ho, William Chan, Chitwan Saharia, Jay Whang, Ruiqi Gao, Alexey Gritsenko, Diederik P Kingma, Ben Poole, Mohammad Norouzi, David J Fleet, et al. Imagen video: High definition video generation with diffusion models. *arXiv:2210.02303*, 2022.
- [31] Jonathan Ho, Tim Salimans, Alexey Gritsenko, William Chan, Mohammad Norouzi, and David J. Fleet. Video diffusion models, 2022.
- [32] Tobias Höppe et al. Diffusion models for video prediction and infilling. *arXiv preprint arXiv:2206.07696*, 2022.
- [33] Vincent Tao Hu et al. Zigma: Zigzag mamba diffusion model. *arXiv preprint arXiv:2403.13802*, 2024.
- [34] Md Mohaiminul Islam and Gedas Bertasius. Long movie clip classification with state-space video models. In *ECCV*, 2022.
- [35] T. Kim, S. Ahn, and Y. Bengio. Variational temporal abstraction. In *Advances in Neural Information Processing Systems*, pages 11566–11575, 2019.
- [36] Diederik P Kingma and Max Welling. Auto-encoding variational bayes. *International Conference on Learning Representations*, 2013.

- [37] Diederik P Kingma, Tim Salimans, Ben Poole, and Jonathan Ho. Variational diffusion models. *arXiv preprint arXiv:2107.00630*, 2021.
- [38] Nikita Kitaev, Lukasz Kaiser, and Anselm Levskaya. Reformer: The efficient transformer. In *International Conference on Learning Representations*, 2020. URL <https://openreview.net/forum?id=rkgNKkHtvB>.
- [39] David M Knigge, David W Romero, Albert Gu, Efstratios Gavves, Erik J Bekkers, Jakub Mikolaj Tomczak, Mark Hoogendoorn, and Jan-jakob Sonke. Modelling long range dependencies in nd: From task-specific to a general purpose cnn. In *International Conference on Learning Representations*, 2023.
- [40] Kunchang Li et al. Videomamba: State space model for efficient video understanding. *arXiv preprint arXiv:2403.06977*, 2024.
- [41] Y. Liu, Y. Tian, Y. Zhao, H. Yu, L. Xie, Y. Wang, Q. Ye, and Y. Liu. Vmamba: Visual state space model. *arXiv preprint arXiv:2401.10166*, 2024.
- [42] Chris Lu, Yannick Schroecker, Albert Gu, Emilio Parisotto, Jakob Foerster, Satinder Singh, and Feryal Behbahani. Structured state space models for in-context reinforcement learning. *arXiv preprint arXiv:2303.03982*, 2023.
- [43] Jun Ma, Feifei Li, and Bo Wang. U-mamba: Enhancing long-range dependency for biomedical image segmentation. *arXiv preprint arXiv:2401.04722*, 2024.
- [44] Harsh Mehta, Ankit Gupta, Ashok Cutkosky, and Behnam Neyshabur. Long range language modeling via gated state spaces. In *The Eleventh International Conference on Learning Representations*, 2023.
- [45] Eric Nguyen, Karan Goel, Albert Gu, Gordon Downs, Preey Shah, Tri Dao, Stephen Baccus, and Christopher Ré. S4nd: Modeling images and videos as multidimensional signals with state spaces. In *Advances in Neural Information Processing Systems*, 2022.
- [46] Alexander Quinn Nichol and Prafulla Dhariwal. Improved denoising diffusion probabilistic models. In *International Conference on Machine Learning*, pages 8162–8171. PMLR, 2021.

- [47] William Peebles and Saining Xie. Scalable diffusion models with transformers. *arXiv preprint arXiv:2212.09748*, 2022. doi: 10.48550/arXiv.2212.09748.
- [48] Robin Rombach, Andreas Blattmann, Dominik Lorenz, Patrick Esser, and Björn Ommer. High-resolution image synthesis with latent diffusion models. In *Proceedings of the IEEE/CVF conference on computer vision and pattern recognition*, pages 10684–10695, 2022.
- [49] Olaf Ronneberger, Philipp Fischer, and Thomas Brox. U-net: Convolutional networks for biomedical image segmentation. In *International Conference on Medical Image Computing and Computer-Assisted Intervention*, pages 234–241. Springer, 2015.
- [50] M. Saito, E. Matsumoto, and S. Saito. Temporal generative adversarial nets with singular value clipping. In *IEEE International Conference on Computer Vision (ICCV)*, 2017.
- [51] Tim Salimans and Jonathan Ho. Progressive distillation for fast sampling of diffusion models. In *International Conference on Learning Representations (ICLR)*, 2022.
- [52] Vaibhav Saxena, Jimmy Ba, and Danijar Hafner. Clockwork variational autoencoders. *Advances in Neural Information Processing Systems*, 34, 2021.
- [53] Zhuoran Shen, Mingyuan Zhang, Haiyu Zhao, Shuai Yi, and Hongsheng Li. Efficient attention: Attention with linear complexities. *CoRR*, abs/1812.01243, 2018. URL <http://arxiv.org/abs/1812.01243>.
- [54] Uriel Singer, Adam Polyak, Thomas Hayes, Xi Yin, Jie An, Songyang Zhang, Qiyuan Hu, Harry Yang, Oron Ashual, Oran Gafni, et al. Make-a-video: Text-to-video generation without text-video data. *arXiv:2209.14792*, 2022.
- [55] Jimmy T.H. Smith, Andrew Warrington, and Scott Linderman. Simplified state space layers for sequence modeling. In *International Conference on Learning Representations*, 2023.

- [56] Jascha Sohl-Dickstein, Eric Weiss, Niru Maheswaranathan, and Surya Ganguli. Deep unsupervised learning using nonequilibrium thermodynamics. In *International Conference on Machine Learning*, pages 2256–2265, 2015.
- [57] Yang Song, Jascha Sohl-Dickstein, Diederik P Kingma, Abhishek Kumar, Stefano Ermon, and Ben Poole. Score-based generative modeling through stochastic differential equations. *arXiv preprint arXiv:2011.13456*, 2021. doi: 10.48550/arXiv.2011.13456.
- [58] Yi Tay, Mostafa Dehghani, Samira Abnar, Yikang Shen, Dara Bahri, Philip Pham, Jinfeng Rao, Liu Yang, Sebastian Ruder, and Donald Metzler. Long range arena: A benchmark for efficient transformers. In *International Conference on Learning Representations*, 2021.
- [59] Sergey Tulyakov, Ming-Yu Liu, Xiaodong Yang, and Jan Kautz. Mocogan: Decomposing motion and content for video generation. In *Proceedings of the IEEE conference on computer vision and pattern recognition*, pages 1526–1535, 2018.
- [60] Thomas Unterthiner, Sjoerd van Steenkiste, Karol Kurach, Raphael Marinier, Marcin Michalski, and Sylvain Gelly. Towards accurate generative models of video: A new metric challenges. *arXiv preprint arXiv:1812.01717*, 2018.
- [61] Ashish Vaswani, Noam Shazeer, Niki Parmar, Jakob Uszkoreit, Llion Jones, Aidan N Gomez, Łukasz Kaiser, and Illia Polosukhin. Attention is all you need. In *Advances in Neural Information Processing Systems*, pages 5998–6008, 2017.
- [62] Vikram Voleti, Alexia Jolicoeur-Martineau, and Chris Pal. Mcvd-masked conditional video diffusion for prediction, generation, and interpolation. In *Advances in neural information processing systems*, volume 35, pages 23371–23385, 2022.
- [63] C. Vondrick, H. Pirsiavash, and A. Torralba. Generating videos with scene dynamics. In *Advances in Neural Information Processing Systems (NeurIPS)*, 2016.

- [64] Jue Wang, Wentao Zhu, Pichao Wang, Xiang Yu, Linda Liu, Mohamed Omar, and Raffay Hamid. Selective structured state-spaces for long-form video understanding. In *CVPR*, 2023.
- [65] Junxiong Wang, Jing Nathan Yan, Albert Gu, and Alexander M Rush. Pretraining without attention. *arXiv preprint arXiv:2212.10544*, 2022.
- [66] Sinong Wang, Belinda Z. Li, Madian Khabsa, Han Fang, and Hao Ma. Linformer: Self-attention with linear complexity, 2020.
- [67] Jing Nathan Yan, Jiatao Gu, and Alexander M Rush. Diffusion models without attention. *arXiv preprint arXiv:2311.18257*, 2023.
- [68] Wilson Yan et al. Videogpt: Video generation using vq-vae and transformers. *arXiv preprint arXiv:2104.10157*, 2021.
- [69] Shengming Yin et al. Nuwa-xl: Diffusion over diffusion for extremely long video generation. *arXiv preprint arXiv:2303.12346*, 2023.
- [70] Daquan Zhou et al. Magicvideo: Efficient video generation with latent diffusion models. *arXiv preprint arXiv:2211.11018*, 2022.
- [71] Linqi Zhou, Michael Poli, Winnie Xu, Stefano Massaroli, and Stefano Ermon. Deep latent state space models for time-series generation. In *International Conference on Machine Learning*, 2023.
- [72] Lianghui Zhu et al. Vision mamba: Efficient visual representation learning with bidirectional state space model. *arXiv preprint arXiv:2401.09417*, 2024.

Appendix A. Experimental Settings

To ensure a fair comparison of the modules extracting the temporal relationships under the same resolution settings, all configurations except for the temporal layers, were the same in our experiments. We used NVIDIA A100 $\times 8$ (from a cloud provider). Hyperparameters, which are consistent across all model sizes and datasets, are shown in Table A.5.

Appendix B. Additional Qualitative Results

Shown in Figure B.7, B.8, B.9.

Table A.5: Hyperparameters used in the experiments.

Parameter	Value
UNet channel multipliers	(1, 2, 4, 8)
Time embedding dimension	1024
Time embedding linears	2
Denoising timesteps (T)	256
Loss type	L2 loss of noise ϵ
Training steps	100k
Optimizer	Adam ($\beta_1 = 0.9$, $\beta_2 = 0.999$)
Learning rate	0.00001
Train batch size	8
EMA decay	0.9999

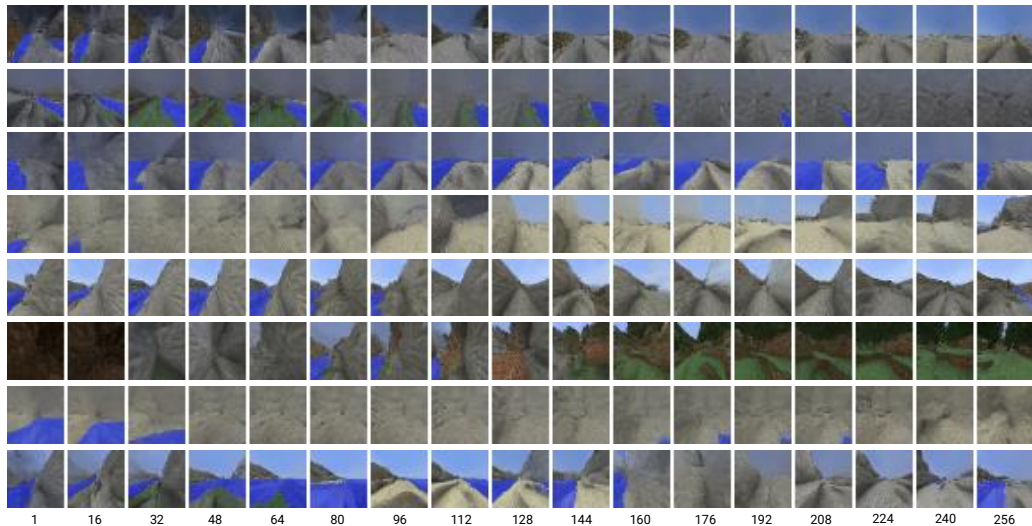


Figure B.7: Additional qualitative generation results in MineRL Navigate (# of frames are 256, 32×32 resolution). Each column represents different samples.

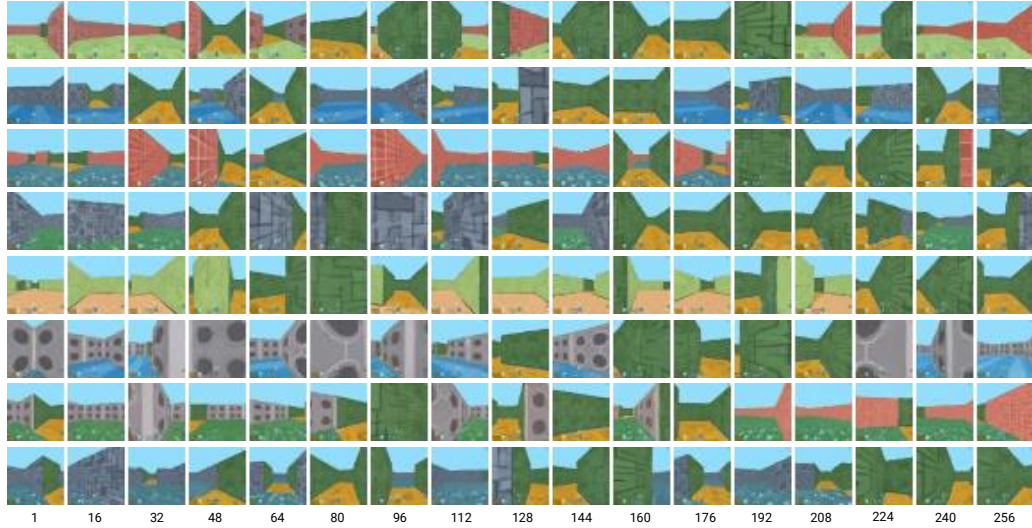


Figure B.8: Additional qualitative generation results in GQN-Mazes (# of frames are 256, 32×32 resolution). Each column represents different samples.

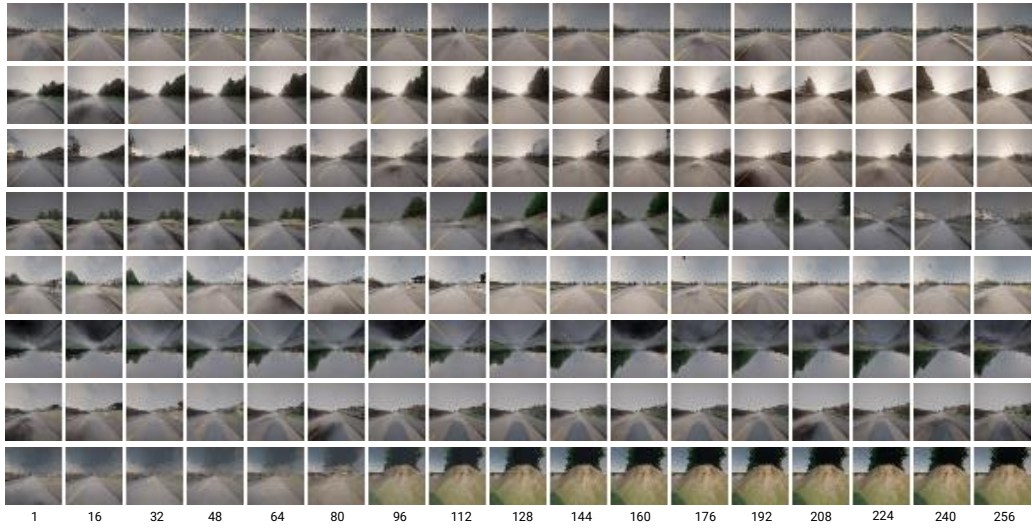


Figure B.9: Additional qualitative generation results in CARLA Town01 (# of frames are 256, 32×32 resolution). Each column represents different samples.